Undersea Biomedical Research, Vol. 16, No. 6, 1989

DTIC
ELECTE
MAR 0 8 1990
S B D
DTIC FILE COPY
(2)

Arterial gas embolism as a pathophysiologic mechanism for spinal cord decompression sickness

AD-A219 769

T. J. R. FRANCIS, G. H. PEZESHKPOUR, and A. J. DUTKA

Diving Medicine Department (T.J.R.F., A.J.D.), Naval Medical Research Institute, Bethesda, Maryland 20814-5055, and Department of Neuropathology (G.H.P.), Armed Forces Institute of Pathology, 6825 16th Street NW, Washington, DC 20306

Francis TJR, Pezeshkpour GH, Dutka AJ. Arterial gas embolism as a pathophysiologic mechanism for spinal cord decompression sickness. Undersea Biomed Res 1989; 16(6):439–451.—A continuous infusion of air (1.0 ml · min^{-1}) was delivered via a fine aortic cannula into the arterial circulation of 7 anesthetized dogs until no spinal cord function could be elicited by somatosensory evoked potentials. The animals were then rapidly perfusion-fixed and the spinal cords removed for histological examination. The appearance of the embolized cords differed substantially from eight spinal cords injured by fulminant decompression sickness (DCS). The embolized cords appeared essentially normal whereas the DCS cords featured extravascular, nonstaining, space-occupying lesions (SOLs) scattered throughout the cord, mainly in the white matter. Two spinal cords injured by DCS with a delayed onset (30 min from surfacing) appeared similar to the embolized cords. These findings are compatible with the hypothesis that two mechanisms are involved in the onset of spinal cord DCS. Fulminant disease is associated with SOLs, which are probably caused by the in situ evolution of a gas phase. Disease with a delayed onset is more likely to be caused by an ischemic mechanism, which in the acute phase is histologically indistinguishable from gas embolism.

central nervous system
bubbles
dysbarism

Ever since decompression sickness (DCS) was first recognized as a disease (1) it has been apparent that involvement of the central nervous system (CNS) is an important feature of the more serious manifestations of the condition (2–5). In particular, spinal cord DCS is a potent cause of both acute and residual morbidity (6).

Unfortunately, despite more than a century of investigation, the mechanisms whereby the spinal cord is injured by DCS remain far from clear. Some of the early attempts to explain the disease were hampered by an inadequate understanding of the laws of physics and physiology (7). More recent hypotheses have developed from the original observation of Boyle (8) that a consequence of rapid decompression is the evolution of a gas phase in blood and tissues.

DISTRIBUTION STATEMENT A
Approved for public release;
Distribution Unlimited

90 03 08 017

A long-standing hypothesis for the mechanism of spinal cord DCS has been based on the proposal that during or shortly after decompression, bubbles of gas appear in the arterial circulation and, acting as emboli, obstruct tissue microcirculation, causing ischemia (2, 9). Possible sources for arterial gas bubbles in DCS include: pulmonary barotrauma (4), bubbles that have nucleated de novo in arterial blood (10), and bubbles from the venous circulation that have either passed through the pulmonary filter (11) or through a right-to-left shunt (such as an atrial septal defect) (12).

A fundamental problem with the embolic-ischemic mechanism is that emboli should be distributed most frequently to highly perfused tissues. Consequently, it is these tissues that might be expected to be most frequently involved in DCS. For example, if DCS is a purely embolic condition the kidneys should be a target organ. However, renal involvement in DCS is extraordinarily rare. With reference to neurologic DCS, Hallenbeck et al. (13) observed that unlike other embolic diseases of the CNS, in which the brain is the principal target organ, it is the spinal cord that seems to be preferentially involved in DCS. They argued that this was difficult to explain on the basis of the distribution of blood flow in the CNS. They proposed an alternative mechanism for spinal cord DCS, which was based on the obstruction of the epidural vertebral venous plexus by bubbles and the products of the biochemical interaction between bubbles and blood.

An alternative means of determining the role of gas embolism in acute spinal cord DCS is to compare the pathology of the two conditions. There is evidence from recent animal studies that acute spinal cord DCS has a distinctive histological appearance. Extravascular, nonstaining, space-occupying lesions (SOLs) have been described that are located principally in white matter (14). There is evidence that they may be a consequence of the in situ liberation of a gas phase (15). Since the histological appearance of acute spinal cord gas embolism has not been described, we undertook this study to compare the two conditions.

METHODS

The following protocol was scrutinized and approved by the Animal Care and Use Advisory Committee of the Naval Medical Research Institute. The experiments were conducted in accordance with the guidelines set forth in the "Guide for the Care and Use of Laboratory Animals," U.S. Department of Health and Human Services publication NIH 86-23, 1985.

Animal preparation

Seven well-conditioned, male mongrel dogs (9.5–13 kg) were sedated with xylazine (2.2 mg · kg^{-1} s.c.) and atropine (0.05 mg · kg^{-1}) before inducing anesthesia with pentobarbital (13.5 mg · kg^{-1} i.v.). Half the induction dose was given 20 min later, and surgical anesthesia was maintained with subsequent doses of pentobarbital (1.3 mg · kg^{-1} i.v.) administered at 20-min intervals. The animals were ventilated, prepared, and monitored in the manner described by Leitch and Hallenbeck (16). In addition, a double-lumen cannula made from PE-10 tubing (INTRAMEDIC) (0.28 mm i.d.) within PE-205 tubing (INTRAMEDIC) (1.57 mm i.d.) was fed through the left femoral artery and located at the arch of the aorta immediately distal to the aortic

Fig. 1. Decompression sickness. A low power cross section of the spinal cord. *Note* the poorly stained, SOL in the white matter *(arrows)*. Pentachrome stain ×4. (Dog 1035, onset 5 min from surfacing.)

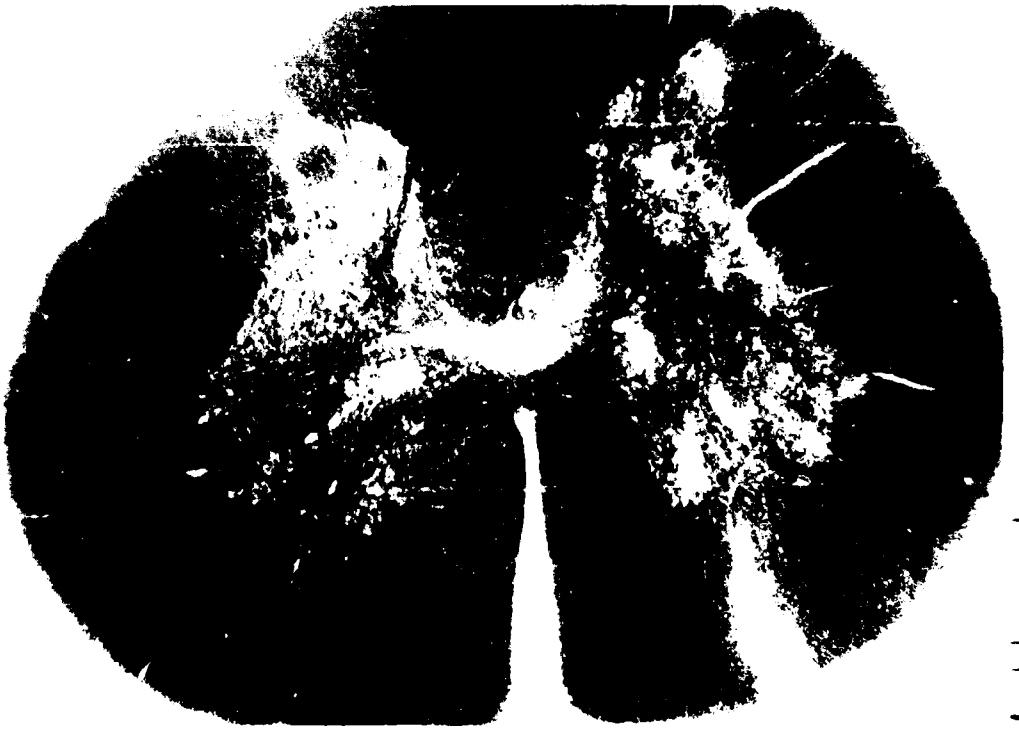

Fig. 2. Gas embolism. Cross section of spinal cord. ×4. There are no poorly stained areas like those in Fig. 1.

Codes
Dist | Avail and/or Special
A-1 | 20

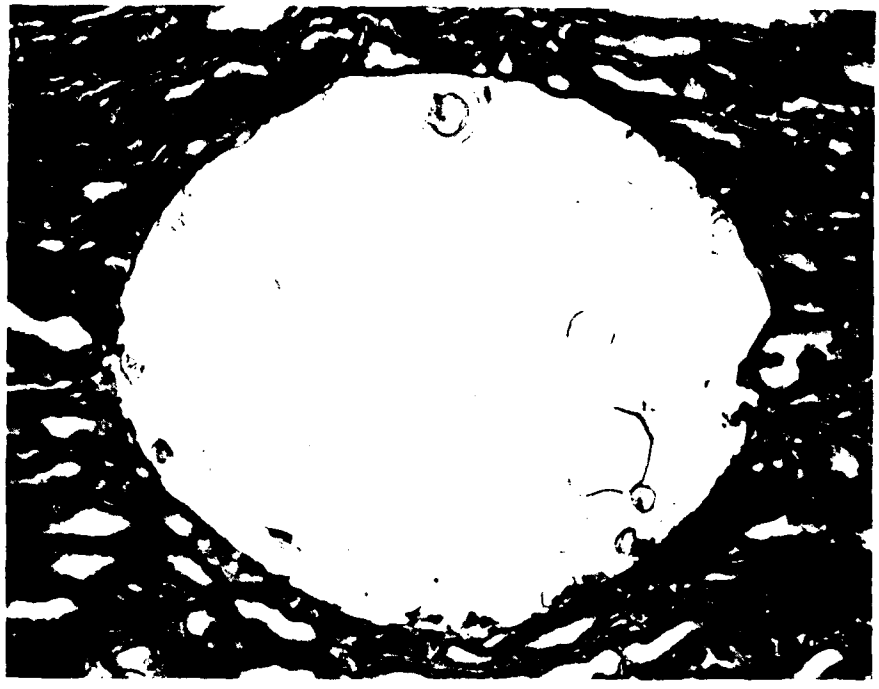

Fig. 3. Decompression sickness. High power LM view of a SOL in longitudinal section. *Note* the distortion of the surrounding axons and the poorly stained cellular debris in the space. Pentachrome stain $\times 180$.

Fig. 4. Decompression sickness. TEM of white matter, uranyl acetate, and lead citrate. $\times 15{,}000$. The figure shows the disruption of white matter architecture.

Fig. 5. Gas embolism. TEM of white matter, uranyl acetate, and lead citrate. ×7000. In the *center* is a blood vessel; *note* the well-preserved perivascular tissue.

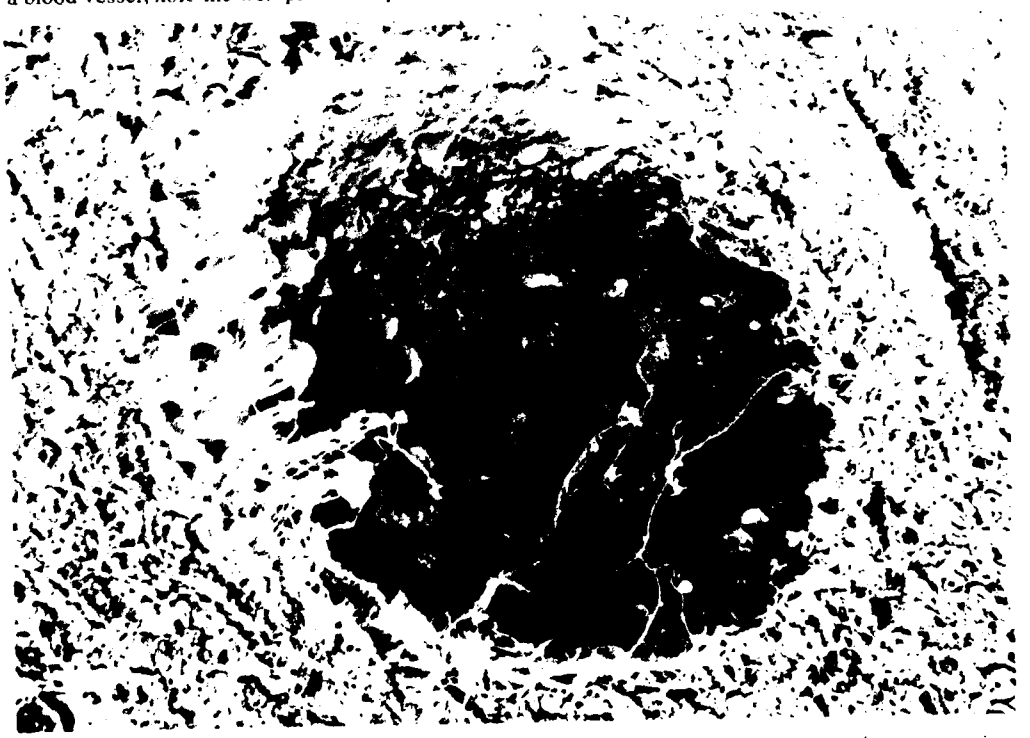

Fig. 6. Decompression sickness. SEM of a SOL showing a debris-strewn crater cut in cross section. ×700.

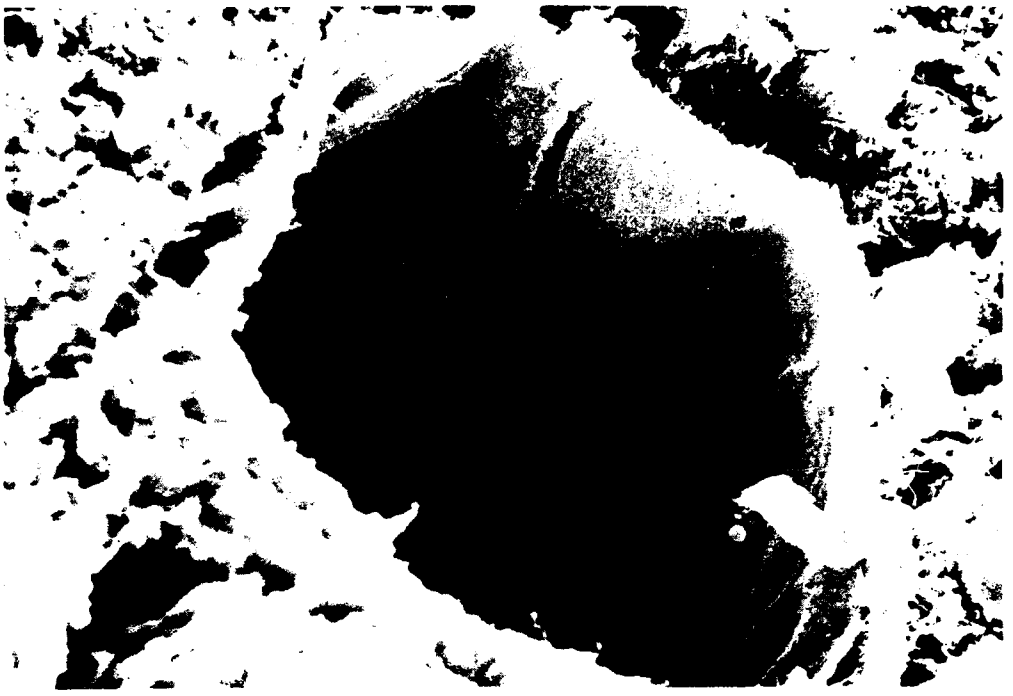

Fig. 7. Decompression sickness. SEM of white matter showing the cut end of a blood vessel, for comparison with Fig. 6. *Note* two erythrocytes adjacent to the cut end of the vessel, the smooth lining of the vessel, and the lack of cellular debris. × 1300.

Fig. 8. Decompression sickness. Cross section of spinal cord (× 4) from a case with a delayed onset (Dog 6909, onset 30 min after surfacing). *Note* the absence of SOLs.

valve. With the outer lumen connected to a pressure transducer (Gould Statham P23 1D), placement of the cannula was confirmed by advancing the tip until a ventricular pressure pattern was recorded and then withdrawing the cannula until the aortic pattern was restored. After preparation the animal was located in a prone position on a stereotactic frame that incorporated a heating pad to allow the maintenance of a stable core temperature.

Somatosensory evoked potentials

Somatosensory evoked potentials (SEP) were recorded from a pair of insulated, 1-mm stainless steel needles introduced percutaneously into the T13/L1 and L1/L2 interspaces and advanced until their tips were firmly embedded in the lamina of the adjacent vertebra. The stimulating electrodes (20-gauge stainless steel needles mounted on a double banana plug) were introduced percutaneously at the level of the head of the fibula to lie adjacent to the peroneal nerve. Evoked potentials were recorded using a Nicolet CA 1000 Clinical Averager. Stimuli of 16 mA and 100 μsec duration were delivered at a rate of 2.9 · sec^{-1}. The signal was filtered (150–3000 Hz bandpass) and recorded for 30 msec with a sensitivity of ± 100 μV and averaged over 84 repetitions. After collection, the SEP were transferred to a Digital PDP 11-70 computer, which determined the summed amplitude (Σa) of the signal (17). Baseline recordings were made from the stimulation of both the left and right peroneal nerves until the amplitude of four consecutive readings varied by no more than 8%. The side that generated the SEP with the greatest amplitude was selected for monitoring throughout the remainder of the experiment.

Spinal cord embolism

The inner element of the double-lumen embolism cannula was connected by a "Y" piece to two 30-ml plastic syringes that were mounted on a pump (Sage Instruments model 355). The pump was set to deliver air into the cannula at a rate of 1.0 ml · min^{-1}.

Following the recording of baseline SEP and other physiologic parameters, the embolism cannula was flushed with normal saline containing heparin 2.0 IU · ml^{-1} and the pump was started. SEP were recorded continuously, and air was infused until the SEP became isoelectric (a Σa of zero) for two consecutive readings. At this stage the animal was removed from the stereotactic frame and prepared for perfusion fixation.

Perfusion fixation

The heart was exposed through a midline thoracotomy. Having reflected the pericardium and with the heart still beating, an 8-mm diameter stainless steel cannula (connected by polyethylene tubing to an Amicon LP-1 peristaltic pump) was introduced into the left ventricle, and fixation commenced with the infusion 3 liters of warm (37°C), heparinized (1 IU · ml^{-1}) normal saline at a rate of 1 liter · min^{-1}. This was immediately followed by 7–8 liters of Karnovsky's solution (pH 7.2, 37°C) delivered at the same rate. Blood, saline, and fixative were drained through a similar cannula located in the right atrium. Throughout fixation every effort was made to avoid introducing further bubbles of gas into the dog. After the infusion of 6 liters of

Karnovsky's solution, each animal was assessed for the completeness of fixation by palpation. Where there existed any residual abdominal softness or lower limb flexibility the fixation was continued by recirculating the remaining fixative. Fixation normally took about 15 min to complete. After fixation the spinal cord was excised through a laminectomy, which was sufficiently extensive to avoid tissue compression or unnecessary flexion during removal. The spinal cord was stored in fresh Karnovsky's solution at 4°C until it was processed for histology.

Histology

The spinal cords were prepared for light microscopy (LM) and transmission electron microscopy (TEM) by first removing the dura mater. The conus was identified and 2-mm slices cut up to the level of T12 (to include the entire portion of the cord interrogated by SEP). The tissue was washed overnight in three to four changes of 0.025 *M* cacodylate buffer (pH 7.4, 4°C) and then postfixed in 2% buffered osmium tetroxide for 2 h. Finally, the slices were dehydrated by sequential immersions in graded alcohol, cleared in propylene oxide, and embedded in an epoxy resin (Polysciences Inc.) (14).

For LM, 2-μm sections were cut and counterstained with multiple stain solution (MSS) (Polysciences Inc.). For TEM, 60–90-nm thin sections were cut with an Ultratome (LKB Instruments), stained with uranyl acetate and lead citrate, and examined by a Zeiss-9 electron microscope.

For scanning electron microscopy (SEM) specimens were first cut and then soaked for 2 h in 2% phosphate buffered glutaraldehyde (pH 7.4). After several washes in the same buffer, containing 0.2 *M* sucrose, the specimens were postfixed for 1 h in buffered 1% OsO_4 (pH 7.4). Each specimen was then dehydrated by passage through graded ethanol and then placed in amyl acetate solution (JT Baker Chemicals, NJ) before drying with liquid CO_2 in a critical point drying chamber at 1200 psi. After mounting on planchets with silver paint, the specimens were coated with 20 nm of gold-palladium in a low-pressure diode sputtering unit. The tissue was examined with a Hitachi S-570 scanning electron microscope operated at 15 kV, and photographs were taken from the record CRT of the microscope with Polaroid P/N 55 film.

Decompression sickness

The histology of the 7 dogs with spinal cord gas embolism was compared with that of 10 dogs given DCS in the manner described by Francis et al. (14). The time to onset of spinal cord dysfunction from gas embolism was compared with the 83 dogs that have developed spinal cord DCS from our standard dive profile. After a preparation similar to the one described above, but with the omission of the embolism cannula, the animals undertook a short, deep chamber dive that was designed to induce spinal cord DCS (18). The profile was a descent to 300 feet of sea water (fsw) at 75 fsw · min^{-1}, followed by 15 min on the bottom and decompression at a rate of 60 fsw · min^{-1} to 60 fsw and at 45 fsw · min^{-1} to the surface. SEP were recorded continuously from the commencement of decompression, and DCS was diagnosed when two consecutive SEP were recorded with an amplitude of less than 80% of the mean baseline value. The animals were perfusion-fixed, and the tissues prepared for histology exactly as described above.

Statistical methods

Comparison of proportions was with the chi-square distribution for 1 degree of freedom with Yates' continuity correction. A result was considered statistically significant if the null hypothesis of equal proportions was rejected on more than 95% of occasions.

RESULTS

Histology

Figure 1 is a representative cross section of a spinal cord rendered dysfunctional within 5 min of surfacing from the DCS-provoking dive. Numerous poorly or completely nonstaining SOLs may be seen. These SOLs are located principally in the white matter. *Arrows* identify particularly good examples. For comparison, Fig. 2 shows a similar representative cross section of a spinal cord rendered dysfunctional by gas embolism. There is an artifactual cut in the white matter to the right side of the photomicrograph, but none of the SOLs so prevalent in Fig. 1 are present. Two features of the SOLs are seen under higher power and longitudinal section in Fig. 3. First, SOLs frequently contain poorly stained cellular debris rather than erythrocytes, which indicates that they are likely to be extravascular. Second, the axons adjacent to the lesions seem to be compressed and distorted. When this observation is considered in the context of the time frame in which these lesions appeared in the cord, it may be implied that they expanded rapidly in size before fixation.

Figure 4 is a transmission electron micrograph of the white matter of a DCS-injured spinal cord. The disruption of myelin is particularly visible. The figure again shows a lesion that is clearly extravascular. By contrast, Fig. 5 shows the tissue surrounding a capillary in the white matter of an embolized spinal cord. A few residual erythrocytes from the perfusion fixation are visible in the intravascular space, and the surrounding tissue is well preserved. This section and higher power views of both white and gray matter show no evidence of mitochondrial or synaptic terminal swelling, which would represent early histological evidence of ischemic injury.

Figures 6 and 7 show cross-sectional views by SEM of the white matter of a cord with DCS. In Fig. 6 the debris-strewn crater of a SOL is featured, the appearance of which is in stark contrast to the relatively smooth endothelial lining of a small blood vessel seen in Fig. 7. This provides further evidence that the SOLs are generally extravascular.

We have found that not all DCS-injured spinal cords demonstrate frequent white matter SOLs. Figure 8, for example, shows a representative, low power cross section of a spinal cord rendered dysfunctional by DCS. We failed to find a SOL in any of the more than 100 sections we examined. An additional DCS cord that we have examined had a similar microscopic appearance. The difference between these cases and the majority of other spinal cords with DCS is that the interval between surfacing and the loss of SEP was long (30 min).

Latency

Figure 9 shows the time taken for gas embolism (at the rate of 1 ml · min^{-1}) to reduce the SEP Σa to 80% of baseline for two consecutive readings. This is directly equivalent to the diagnostic criterion used for determining the onset of spinal cord DCS. The embolism latency data are plotted with the time to diagnosis of spinal cord DCS for 83 animals that undertook the 300-fsw dive profile. Gas embolism took significantly longer to reduce SEP amplitude than DCS. The median time to onset of DCS was 6 min, by which time none of the embolized animals showed evidence of spinal cord dysfunction ($\chi^2 = 5.29$, $P < 0.05$).

An average of 26.3 ml ± 7.2 (SD) of injected gas was required to extinguish the SEP of the embolized animals. Since the mean time from commencing embolism to diagnosis was 16 min, it may be seen that there was a delay of about 10 min between the onset of spinal cord dysfunction and the SEP becoming isoelectric.

DISCUSSION

We have found that the acute histological appearance of the spinal cord immediately after the onset of DCS and gas embolism is usually different. When there is a rapid loss of function due to DCS, which is the most common presentation in this model (Fig. 9), we have found nonstaining SOLs scattered throughout the white matter (Fig. 1). The evidence from Figs. 3, 4, and 6 is that these lesions are extravascular and are not found in spinal cords rendered nonconducting by gas embolism (Figs. 2 and 5). In fact, no abnormalities were seen in the embolized cords. This is not entirely surprising because the earliest histological evidence of ischemia, the swelling of synaptic terminals and mitochondria, takes 30–60 minutes to develop from the onset of the ischemic insult. The spinal cords in this experiment were fixed before such changes were likely to develop.

The histological findings in spinal cord DCS are not uniform. In 2 animals, which experienced a delay of 30 min between surfacing from the dive and the loss of SEP amplitude, SOLs were rarely seen and the cords had a histological appearance that was indistinguishable from gas embolism (Fig. 8).

Another observation is that the loss of spinal cord function occurred significantly more rapidly in dogs injured by DCS than by gas embolism. It is possible that this was due to our choice of the rate of gas infusion. Although an injection of gas into the aorta at a rate equivalent to 7 ml · min^{-1} would prove rapidly fatal in man, this may underrepresent the release of gas into the arterial blood stream in dogs undergoing this dive profile. Nonetheless, we believe that it is unlikely that gas embolism at any rate would disable the spinal cord as rapidly as is possible in DCS. We have previously demonstrated, for example, that there is no significant difference in the time taken for the SEP to become isoelectric in dogs with DCS from this dive profile and dogs with complete spinal cord ischemia due to clamping the aorta (14).

We have evidence, therefore, for two different processes occurring in the spinal cord that may result in a loss of function after a dive. The first is associated with a rapid onset and the presence of SOLs in histological sections, and the second is associated with a delayed onset and normal acute histology. This latter presentation is compatible with a gas embolism mechanism.

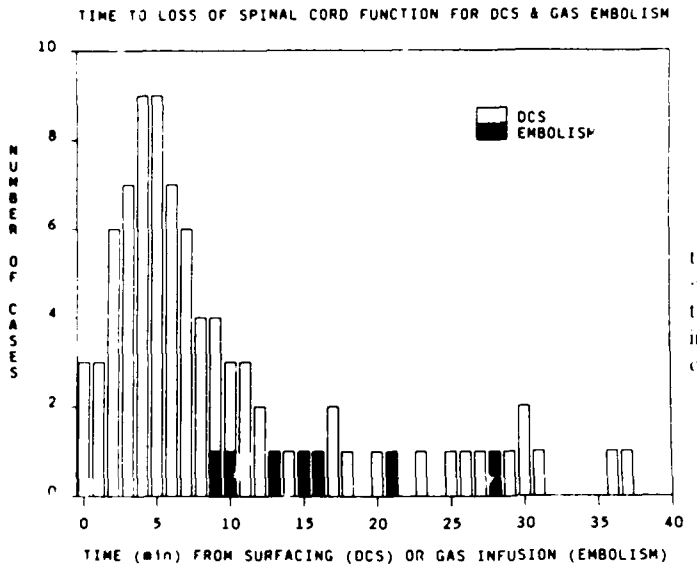

Fig. 9. A histogram showing the time to diagnosis (SEP amplitude < 80% of baseline for 2 consecutive readings) of 83 cases of experimental spinal cord DCS and 7 cases of spinal cord gas embolism.

One of the principal reasons why Hallenbeck et al. (13) argued against gas embolism as a mechanism for spinal cord DCS is that historically the spinal cord appeared to be clinically involved in CNS DCS more frequently than the brain. This is the reverse of what would be expected based on the distribution of blood flow and emboli. For gas embolism to be the mechanism for CNS DCS it would be necessary to postulate extensive yet clinically "silent" cerebral injury. With the use of modern investigative techniques evidence is now emerging that the brain may be involved to a greater extent than is apparent from clinical examination alone. Single photon emission tomography studies of the victims of diving accidents show unexpectedly extensive areas of cerebral hypoperfusion (19, 20). In another recent study it is postulated that ocular fundus lesions, which have been detected in divers, represent evidence of damage by bubble emboli (21). Further evidence for the role of gas embolism in CNS DCS has come from contrast echocardiographic studies of diving accident victims. Moon et al. (12, 22) have demonstrated a significantly higher incidence of atrial septal defects in cases of DCS with CNS involvement than in a group of divers with pain-only bends and a population of "normal" controls. It should be noted, however, that the great majority of the cases they studied with neurologic DCS had cerebral rather than spinal cord symptoms (Moon RE, personal communication).

These recent studies provide evidence that gas embolism may play an important role in the pathogenesis of cerebral DCS. The role of gas emboli in spinal cord DCS, however, is not so clear. It is well recognized that the pathology of chronic spinal cord DCS is of white matter gliosis, demyelination, and secondary tract degeneration with subpial sparing (23–29). This is at variance with the appearance of primarily gray matter lesions seen in animal models of spinal cord embolism and ischemia (30, 31). It was the overwhelming involvement of spinal cord white matter that led Boycott et al. (32) to modify the simple embolic-ischemic mechanism. They proposed that although bubble emboli are distributed to all tissues, it is only the microcirculation of lipid-rich tissues that becomes obstructed. They reasoned that in aqueous tissues, which contain a relatively low inert gas concentration, bubble emboli grow insuffi-

ciently to obstruct the microcirculation before transiting to the venous drainage. On the other hand, in lipid-rich tissues containing a relatively high inert gas concentration the bubble emboli grow sufficiently to obstruct the microcirculation. Such a mechanism would adequately explain the chronic histological features of spinal cord DCS, but simple obstruction of the white matter microcirculation is inadequate to explain the presence of extravascular SOLs in acute histological sections. Furthermore, the kinetics of the loss of spinal cord function in rapidly progressive forms of DCS also mitigates against a purely embolic-ischemic mechanism.

In conclusion therefore we have shown that gas embolism may result in spinal cord dysfunction. This may be the mechanism of spinal cord DCS in cases where there is a delayed onset of symptoms or where there is concurrent overt or clinically silent cerebral involvement. It is more difficult to implicate gas embolism as a mechanism for spinal cord DCS where there is a rapid onset of symptoms following the hyperbaric exposure, where there is no evidence of cerebral involvement, or where there is histological evidence of predominantly white matter injury.

We gratefully acknowledge the professional skill and kind assistance of E. Sloan, C. Jones, M. Routh, and J. Valesquez during the conduct of the experiments and I. Valenzuela for his expertise in preparing the tissue for histology. The editorial contribution of S. Cecire and J. Gaines is also much appreciated.

This work was supported by the Naval Medical Research and Development Command Work Unit No. 63713N M0099.01C 1007. This manuscript was prepared by United States Government employees as part of their official duties and, therefore, cannot be copyrighted and may be copied without restriction.

The opinions expressed herein are the private ones of the authors and are not to be construed as official or reflecting the views of the U.S. Navy, the Royal Navy, or the naval service at large.

Presented in part at the Undersea and Hyperbaric Medical Society Annual Scientific Meeting, Honolulu, HI, 6–11 June 1989.—*Manuscript received May 1989; accepted June 1989.*

REFERENCES

1. Pol B, Watelle TH. Memoir sur les effets de la compression de l'air applique au creusement des puids a houille. Ann d'Hyg. pub et med legale. Paris. 1854; Ser 2(1):241–279.
2. Bert P. Barometric pressure. Researches in experimental physiology. Translated from the French by Hitchcock MA, Hitchcock FA. Bethesda, MD: Undersea Medical Society Inc, 1978.
3. Behnke AR. Decompression sickness following exposure to high pressures. In: Fulton JF, ed. Decompression sickness. Philadelphia: WB Saunders Co, 1951:53–89.
4. Golding FL, Griffiths P, Hempleman HV, Paton WDM, Walder DN. Decompression sickness during the construction of the Dartford Tunnel. Br J Ind Med 1960; 17:167–180.
5. Erde A, Edmonds C. Decompression sickness: a clinical series. J Occup Med 1975; 17:324–328.
6. Miller JN, Parmentier JL, et al. Rehabilitation of the paralyzed diver. Proceedings of the Thirtieth Undersea Medical Society Workshop. Bethesda, MD: Undersea Medical Society Inc., 1985.
7. Van Rensenlaer H. The pathology of caisson disease. Med Rec New York 1891; 40:141–150.
8. Boyle R. New pneumatical experiments about respiration. Philos Trans R Soc 1670; 5:2035–2056.
9. Hill L, Macleod JJR. Caisson illness and diver's palsy. An experimental study. J Hyg (Cambridge) 1903; 3:401–445.
10. Hills BA. Decompression sickness, vol. 1. Chichester, England: John Wiley & Sons, 1977:65.
11. Butler BD, Hills BA. Transpulmonary passage of venous air emboli. J Appl Physiol 1985; 59:543–547.
12. Moon RE, Camporei EM, Kissle JA. Patent foramen ovale and decompression sickness in divers. Lancet 1989; 513–514.
13. Hallenbeck JM, Bove AA, Elliott DH. Mechanisms underlying spinal cord damage in decompression sickness. Neurology 1975; 25:308–316.
14. Francis TJR, Pezeshkpour GH, Dutka AJ, Hallenbeck JM, Flynn ET. Is there a role for the autochthonous bubble in the pathogenesis of spinal cord decompression sickness? J Neuropathol Exp Neurol 1988; 47:475–487.

15. Burns BA, Hardman JM, Beckman EL. In situ bubble formation in acute central nervous system decompression sickness. J Neuropathol Exp Neurol 1988; 47.371.
16. Leitch DR, Hallenbeck JM. Oxygen in the treatment of spinal cord decompression sickness. Undersea Biomed Res 1985; 12:269–289.
17. Francis TJR, Dutka AJ. Methyl prednisolone in the treatment of acute spinal cord decompression sickness. Undersea Biomed Res 1989; 16:165–174.
18. Leitch DR, Hallenbeck JM. A model of spinal cord dysbarism to study delayed treatment: I. Producing dysbarism. Aviat Space Environ Med 1984; 55:584–591.
19. Macleod MA, Adkisson GA, Fox MJ, Pearson RR. ^{99m}Tc^{m}-HMPAO single photon emission tomography in the diagnosis of cerebral barotrauma. Br J Radiol 1988; 61:1106–1109.
20. Adkisson GA, Macleod MA, Hodgson M, et al. Cerebral perfusion deficits in dysbaric illness. Lancet 1989; 15 July:119–122.
21. Polkinghorne PJ, Sehmi K, Cross MR, Minassian D, Bird AC. Occular fundus lesions in divers. Lancet 1988; 17 Dec:1381–1383.
22. Moon RE, Camporesi EM, Kisslo JA. The relationship between right-to-left shunt and decompression sickness: an update. Undersea Biomed Res 1989; 16(Suppl):91.
23. Heller R, Mager W, von Schrotter H. Luftdruckerkrankungen mit besonderer berucksichtigung der sogenannten caissonkrankheit. Vienna: Alfred Holder, 1900.
24. Lichtenstein GW, Zeitlin H. Caisson disease. A histologic study of late lesions. Arch Pathol 1936; 22:86–98.
25. Palmer AC, Blakemore WF, Greenwood AG. Neuropathology of experimental decompression sickness (dysbarism) in the goat. Neuropathol Appl Neurobiol 1976; 2:145–156.
26. Palmer AC, Calder IM, McCallum RI, Mastaglia FL. Spinal cord degeneration in a case of "recovered" spinal DCS. Br Med J 1981; 283:888–889.
27. Palmer AC. The neuropathology of decompression sickness. In: Cavanagh JB, ed. Recent advances in neuropathology, no 3. Edinburgh: Churchill Livingstone, 1986:141–147.
28. Calder IM. Dysbarism. A review. Forensic Sci Intl 1986; 30:237–266.
29. Kitano M, Kayashi K, Kanoshima M, Tokofuji S, Yamaguchi A. Late manifestation of spinal cord lesions in decompression sickness: histopathologic analysis of an autopsy case. In: Bove AA, Bachrach AJ, Greenbaum LJ, eds. Underwater and hyperbaric physiology IX. Proceedings of the ninth international symposium on underwater and hyperbaric physiology. Bethesda, MD: Undersea and Hyperbaric Medical Society, 1987.
30. Finlayson MH, Mesereau WA, Moore S. Spinal cord emboli in dogs and monkeys and their relevance to aortic atheroma in man. J Neuropathol Exp Neurol 1972; 31:535–547.
31. DeGirolami U, Zivin JA. Neuropathology of experimental spinal cord ischemia in the rabbit. J Neuropathol Exp Neurol 1982; 41:129–149.
32. Boycott AE, Damant CCC, Haldane JS. Prevention of compressed air illness. J Hyg (Cambridge) 1908; 8:342–443.